IRSTI 44.31.41; 30.17.35 10.26577/ijmph.202617111

Performance Evaluation of Three Types of Air-to-Water Cascade Heat Pumps for Cold Climate Applications Using Different Refrigerant Pairs

Ye. Rymkul [1,2], **Ye. Yerdesh** [1,2], **A. Toleukhanov** [2], **Ye. Belyayev** [1,2], **M. Mohanraj** [3], **H.S. Wang** [4], **O. Botella** [5] **and M. Feidt** [5]

[1] *Farabi University, 71 al-Farabi ave., 050040, Almaty, Kazakhstan*
[2] *Department of Mechanical Engineering, Satbayev University, 22a Satbayev str., 050013, Almaty, Kazakhstan*
[3] *Department of Mechanical Engineering, Hindusthan College of Engineering and Technology, Coimbatore 641032, India*
[4] *School of Engineering and Materials Sciences, Queen Mary University of London, UK*
[5] *Universite de Lorraine, CNRS, LEMTA, F-54000 Nancy, France*

Email: yerzhan.belyaev@kaznu.edu.kz; yerzhan.belyayev@gmail.com

(Received 30 April 2026; revised 19 May 2026; accepted 30 May 2026)

Abstract. The performance of conventional air-to-water heat pumps significantly deteriorates at low ambient temperatures due to high temperature lift and compressor limitations. This study investigates the thermodynamic performance of three cascade air-to-water heat pump configurations for cold climate applications using sixteen refrigerant pairs. A numerical model was developed in Python using CoolProp for thermophysical properties, considering ambient temperatures down to -50 °C and a heating supply temperature of +60 °C. The results indicate that R32/R134a and R410A/R134a achieve the highest COP, reaching up to 2.56 at +10 °C and approximately 1.98 at -30 °C; however, their operation is limited by environmental constraints and operating range. R744-based systems enable operation at extreme low temperatures down to -41 °C, with COP values of 1.62 (R744/R134a) and 1.60 (R744/R290). Among the configurations, the first and third show the highest efficiency (COP ≈ 2.0), while the second exhibits a ∼4.6% lower COP but offers operational flexibility, including single-stage operation above -10 °C. Considering both performance and environmental impact, R744/R290 is identified as the most promising refrigerant pair for future applications.

Keywords: Cascade heat pump; cold climate; COP; pressure ratio; environmentally friendly refrigerant.

Introduction

The transition toward low-carbon and energy-efficient heating technologies has become one of the major global priorities due to increasing energy consumption, greenhouse gas emissions, and the need to reduce dependency on fossil fuels [1]. The building sector accounts for a significant share of total global energy demand, where space heating and domestic hot water production remain the dominant contributors to energy consumption in cold climate regions [2]. Heat pump technologies are therefore considered one of the most promising solutions for sustainable heating applications because of their high energy efficiency and potential for electrification of heating systems [3, 4].

Among various heat pump technologies, air-to-water heat pumps (AWHPs) have attracted considerable attention because of their relatively simple installation, low initial investment compared to ground-source systems, and wide applicability in residential and industrial sectors [5]. However, conventional single-stage air-to-water heat pumps experience serious performance degradation under low ambient temperature conditions [6]. In continental and severe winter climates, such as those observed in Kazakhstan, Northern Europe, Canada, and other cold regions, the outdoor air temperature may decrease below -20 °C, causing substantial reductions in heating capacity and coefficient of performance (COP) [7]. In addition, the compressor discharge temperature significantly increases under large temperature lift conditions, which limits the operational reliability and efficiency of conventional vapor compression systems [8, 9].

To overcome these limitations, cascade heat pump systems [6, 7] have emerged as an effec-

tive technological solution for high-temperature [9] heating applications under cold climate conditions. A cascade heat pump consists of two interconnected vapor compression cycles operating with different refrigerants through an intermediate cascade heat exchanger [6, 7]. Such a configuration allows the system to achieve higher condenser temperatures while maintaining moderate compression ratios and improved thermodynamic performance. Cascade systems are especially suitable for domestic hot water production, industrial heating processes, and district heating applications requiring supply temperatures above 60-70 °C [9, 10, 11].

The selection of refrigerant pairs plays a critical role in the thermal and environmental performance of cascade heat pump systems. Different refrigerant combinations strongly influence the heating capacity, compressor work, pressure ratio, discharge temperature, volumetric heating capacity, exergy destruction, and overall system COP. In recent years, considerable attention has been devoted to the replacement of conventional high-global-warming-potential (GWP) refrigerants with environmentally friendly alternatives due to increasingly strict environmental regulations. Refrigerants such as R290, R1234yf, R744, R134a, R410A, and their combinations have been investigated in cascade systems to improve both thermodynamic efficiency and environmental sustainability [6, 7].

Several previous studies investigated the thermodynamic behavior of cascade heat pump systems using different refrigerant pairs. Yerdesh et al. [6, 7] analyzed the thermal performance of an air-to-water cascade heat pump operating under continental climate conditions and demonstrated that cascade configurations can effectively provide condenser temperatures above 70 °C while maintaining stable operation at low ambient temperatures. Other researchers evaluated the feasibility of cascade heat pump systems for simultaneous indoor heating and domestic hot water production in retrofitted buildings and highlighted the advantages of cascade operation for building electrification strategies [12, 13, 14, 15, 16, 17]. Boahen et al. [12] investigated the performance characteristics of a water-to-water cascade multifunctional heat pump system designed for space heating, domestic hot water production, and simultaneous operation under winter conditions. Their analysis, conducted over a range of secondary fluid temperatures, demonstrated that cascade multifunctional configurations can achieve improved energy efficiency at elevated heating and hot water demands. The study further highlighted the capability of such systems to effectively meet simultaneous space heating and domestic hot water requirements during the heating season, making them particularly attractive for cold climate applications. Zhang et al. [15] investigated the performance of an R134a/CO_2 cascade air-source heat pump system under cold climate conditions in China. Their experimental results demonstrated that the proposed system is capable of supplying hot water at temperatures above 50 °C while maintaining relatively high energy performance. Specifically, the system achieved coefficients of performance (COP) of up to 3.07 at an ambient temperature of -5 °C and 1.60 at -45 °C. These findings highlight the suitability of cascade configurations for reliable high-temperature heating applications in severe cold environments. Ma et al. [18] proposed a novel air-source cascade steam-generating heat pump capable of producing high-temperature steam up to 170 °C from low-grade heat sources ranging from -30 °C to 80 °C. Their study demonstrated stable operation under cold climate conditions, with a COP of about 1.42 at -30 °C, highlighting the potential of cascade configurations for large temperature lift applications and industrial decarbonization. Wu et al. [19] investigated the experimental performance and industrial application of a cascade air-source high-temperature heat pump, demonstrating its capability to supply hot water up to 120-125 °C with a COP of about 1.7-1.8. Their results confirmed stable operation and practical feasibility in real industrial conditions, highlighting the potential of cascade configurations for replacing conventional boilers in high-temperature heating applications. Furthermore, previous investi-

gations showed that cascade systems can reduce excessive compressor discharge temperatures and improve system reliability compared to single-stage cycles under large temperature lift conditions [1, 2, 3, 4]. Despite the growing number of studies on cascade heat pump technologies, comparative investigations of different types of air-to-water cascade heat pump configurations operating with various refrigerant pairs under cold climate conditions remain limited. In particular, there is still insufficient understanding regarding the comparative thermodynamic performance, heating characteristics, and operational limitations of different cascade cycle configurations under identical operating conditions. Moreover, the influence of refrigerant pair selection on system efficiency and environmental performance requires further detailed investigation for practical implementation in severe winter regions. Therefore, the present study aims to perform a comprehensive thermodynamic performance evaluation of three different types of air-to-water cascade heat pump systems for cold climate applications using various refrigerant pairs. The study focuses on the analysis of heating capacity, coefficient of performance, compressor work, discharge temperature, and overall thermodynamic behaviour under low ambient temperature conditions. The obtained results are expected to contribute toward the development of efficient and environmentally friendly cascade heat pump technologies suitable for sustainable heating applications in continental climate regions. The novelty of this study lies in the comparative thermodynamic evaluation of three air-to-water cascade heat pump configurations using sixteen refrigerant pairs under identical operating conditions and ambient temperatures down to -50 °C. The results identify the most promising refrigerant pairs and system configurations for efficient and environmentally friendly heating in severe continental climates.

System Description

The proposed system is an air-to-water cascade heat pump developed as a part of a cascade heat pump system for space heating and domestic hot water production in continental climate regions. The system is intended for low outdoor air temperatures, where a conventional single-stage vapour compression heat pump has a limited temperature lift and reduced efficiency. To increase the useful heat delivery temperature, two vapour compression cycles are connected in series: a low-temperature (LT) cycle and a high-temperature (HT) cycle.

The LT cycle extracts heat from the outdoor air through an air-source evaporator. After evaporation, the refrigerant vapour is compressed and transfers heat to the HT cycle through an intermediate heat exchanger. The HT cycle absorbs this heat, compresses the refrigerant to a higher pressure and temperature level, and rejects useful heat to the heating circuit. Both cycles include the main components of a vapour compression heat pump: compressor, compact brazed plate heat exchanger, thermostatic expansion valve and evaporator. The prototype also includes liquid receivers, sight glasses, filter driers, pressure gauges, pressure cut-outs, circulation pumps, a control panel and a hot water storage tank. The experimental air-to-water cascade heat pump prototype was assembled for the R410A/R134a refrigerant pair due to the availability of compatible components.

The first configuration (Fig. 1) is the basic air-to-water cascade heat pump. It consists of two closed vapour compression circuits connected in series through a compact brazed plate heat exchanger. In the LT cycle, the refrigerant vapour at point 1 is sucked by the first compressor. After compression, the refrigerant at high pressure and temperature reaches point 2 and enters the condenser, which also acts as the intermediate heat exchanger between the two cycles. In this heat exchanger, the LT refrigerant releases heat to the refrigerant of the HT cycle.

After condensation, the LT refrigerant passes through the liquid receiver, sight glass and filter drier, and then enters the thermostatic expansion valve. After throttling, the two-phase refrigerant at point 4 enters the air-source evaporator, absorbs heat from the ambient air and returns to the com-

pressor.

In the HT cycle, the refrigerant heated in the intermediate heat exchanger reaches point 5 and is compressed by the second compressor. It then rejects useful heat in the condenser connected to the hot water storage tank. Thus, the intermediate heat exchanger simultaneously operates as the condenser of the LT cycle and as the evaporator of the HT cycle.

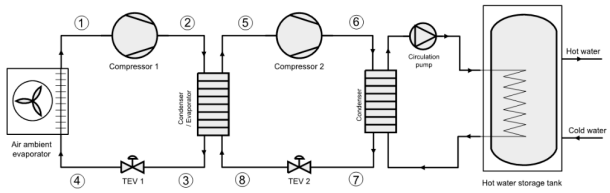

Figure 1 - Scheme of the air-to-water cascade heat pump in the first configuration.

The second configuration (Fig. 2) introduces an intermediate heat transfer circuit between the LT and HT vapour compression cycles. In this arrangement, the system can be considered as a serial connection of an air-to-water heat pump and a water-to-water heat pump. The LT cycle rejects heat to an intermediate heat transfer fluid, and this fluid then supplies heat to the evaporator of the HT cycle. Therefore, the LT condenser and the HT evaporator are separated by an intermediate liquid loop rather than being combined in one refrigerant-to-refrigerant heat exchanger.

The main advantage of this configuration is the convenience of assembly, installation and adjustment. The block-type connection of the two heat pump stages makes the system more flexible for experimental testing and practical application. At sufficiently high ambient temperatures, the system can be operated with one of the cycles disconnected, which reduces electricity consumption during autumn and spring periods. The drawback of this layout is the additional temperature difference introduced by the intermediate heat transfer loop, which slightly reduces the COP compared with the direct cascade arrangement.

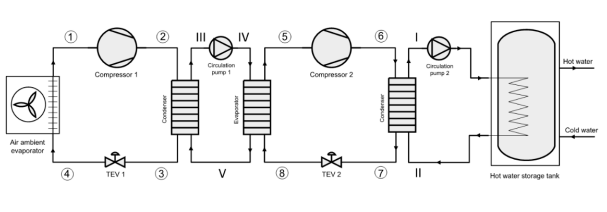

Figure 2 - Scheme of the air-to-water cascade heat pump in the second configuration.

The third configuration (Fig. 3) is a modified cascade system with an additional air-source evaporator installed in the HT cycle. Compared with the second configuration, this layout does not use an intermediate heat transfer fluid circuit between the two refrigerant cycles. Instead, the operating mode is changed by three-way valves, which allow the HT cycle either to receive heat from the LT cycle through the condenser-evaporator heat exchanger or to operate directly with the additional air-source evaporator.

In the full cascade mode, the additional air-source evaporator is blocked by the three-way valve. The HT refrigerant receives heat from the LT cycle through the condenser-evaporator heat exchanger, and both compressors operate together. This mode is intended for low ambient temperatures, when the required temperature lift cannot be efficiently achieved by a single-stage cycle. In the single-stage mode, the LT vapour compression cycle is switched off and the three-way valve blocks the connection with the LT cycle. The HT cycle then operates as a conventional air-source heat pump using the additional air-source evaporator. This mode is suitable at outdoor air temperatures of about -10 °C and above. This operating strategy avoids unnecessary operation of both compressors under moderate ambient conditions and improves seasonal energy performance.

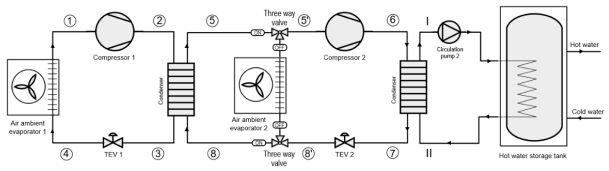

Figure 3 - Scheme of the air-to-water cascade heat pump in the third configuration.

The pressure-enthalpy diagram corresponding to cascade operation is presented in Fig. 4. State points 1-4 describe the LT cycle: compressor suction, compressor discharge, condenser outlet and expansion valve outlet, respectively. State points 5-8 describe the same processes in the HT cycle: compressor suction, compressor discharge, condenser outlet and expansion valve outlet. Therefore, processes 1-2 and 5-6 correspond to compression, 2-3 and 6-7 to condensation, 3-4 and 7-8 to throttling, and 4-1 and 8-5 to evaporation.

In the present study, the system is analysed mainly in cascade operation mode. The dual-mode capability of the third configuration is considered as a design feature aimed at improving seasonal performance under variable outdoor air temperatures. The proposed configurations make it possible to compare direct cascade coupling, intermediate heat transfer coupling and single-stage switching as alternative layouts for an air-to-water cascade heat pump in continental climate conditions.

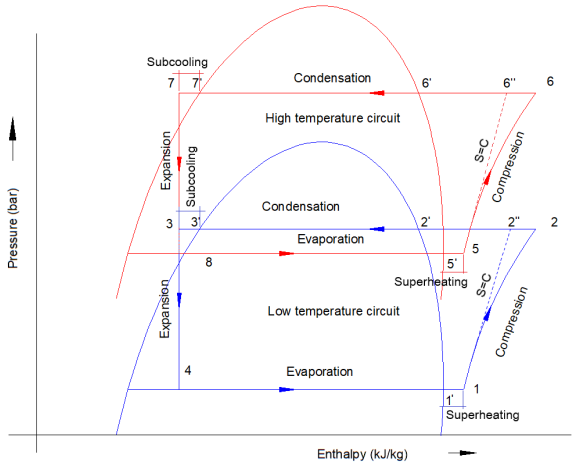

Figure 4 - Pressure-enthalpy diagram of the cascade heat pump cycle.

Mathematical Model

The thermal performance of the cascade air-to-water heat pump was projected using a numerical model developed in Python. The thermophysical properties of the selected refrigerant pairs were obtained from the CoolProp library, which was used to determine enthalpy, entropy, pressure, temperature and saturation properties at the main state points of the cycle. The input parameters were chosen according to the meteorological conditions of Astana, Kazakhstan. The heat output of the cascade system was calculated for the refrigerant pairs presented at the end of this section. State points 1, 2, 3 and 4 in Fig. 4 represent compressor suction, compressor discharge, condenser outlet and expansion valve outlet in the low-temperature cycle, respectively. State points $3'$ and $1'$ correspond to the refrigerant conditions after subcooling and superheating. Similarly, state points 5, 6, 7 and 8 describe compressor suction, compressor discharge, condenser outlet and expansion valve outlet in the high-temperature cycle, points $7'$ and $5'$ characterize the conditions after subcooling and superheating. These parameters are used to define the heat transfer processes and close the thermodynamic model. The following assumptions are considered for the modelling of the cascade air-source heat pump:

1. The refrigerant compression processes are accepted to be isentropic [3].
2. The condensation of refrigerant in the condensers and evaporators of both refrigeration cycles are accepted to be constant pressure processes [3].
3. The refrigerant expansion in an expansion valve is assumed as isenthalpic [4].
4. The pressure losses in the suction and discharge of both low and high temperature compressor are neglected.
5. Compression processes isentropic efficiencies are considered according to [20] and [21].
6. Compressors electric motor efficiencies are assumed to be 0.85 [22].
7. Compressors mechanical efficiencies are assumed to be 0.95 [22].

In addition, other model parameters, such as the degree of subcooling (SC) in the condenser

and superheating (*SH*) in the evaporator, as well as the approach temperature differences (*CAT*) in the evaporator and condenser [23], were set according to Ref. [7].

The heat gain by the ambient-source evaporator is provided by [24]:

$$\dot{Q}_{\text{evap,LT}} = \dot{m}_{\text{ref,LT}}(h_1 - h_4). \tag{1}$$

The low-temperature (LT) cycle compression power is provided by the following equations [20]:

$$\dot{W}_{\text{comp,LT}} = \dot{m}_{\text{ref,LT}}(h_2 - h_1), \tag{2}$$

$$\dot{W}_{\text{comp,LT}} = \frac{\dot{m}_{\text{ref,LT}}(h_{2s} - h_1)}{\eta_{\text{isen,LT}}}, \tag{3}$$

$$\eta_{\text{isen,LT}} = 0.98\left(\frac{T_{1'}}{T_{3'}}\right). \tag{4}$$

Eq. (2) defines the actual compression 1-2 according to Fig. 4. Alternatively, Eq. (2) can be stated in terms of Eqs. (3) and (4), where the numerator of Eq. (3) describes ideal compression 1-2" according to Fig. 4, with the assumption of an adiabatic process [25]. Division by the isentropic efficiency gives the actual compression [4].

The LT cycle compressor power consumption is given by:

$$\dot{W}_{\text{elec,LT}} = \frac{\dot{W}_{\text{comp,LT}}}{\eta_m \eta_t \eta_{\text{elec}}}, \tag{5}$$

$$\dot{W}_{\text{comp,total}} = \dot{W}_{\text{comp,HT}} + \dot{W}_{\text{comp,LT}}, \tag{6}$$

where η_m is the mechanical efficiency of the compressor, which is equal to 0.85; η_t is the efficiency of transmission between the electric motor and the compressor, where for direct coupling it is equal to 1.0 [25]; and η_{elec} is the compressor electric motor efficiency, which is equal to 0.95.

For the high-temperature (HT) cycle compression, the same approach is used as for the LT cycle, Eqs. (2)-(5), leading to the following formulas:

$$\dot{W}_{\text{comp,HT}} = \dot{m}_{\text{ref,HT}}(h_6 - h_5), \tag{7}$$

$$\dot{W}_{\text{comp,HT}} = \frac{\dot{m}_{\text{ref,HT}}(h_{6s} - h_5)}{\eta_{\text{isen,HT}}}, \tag{8}$$

$$\eta_{\text{isen,HT}} = 0.98\left(\frac{T_{5'}}{T_{7'}}\right). \tag{9}$$

The total system power consumption is evaluated using the following equation [26]:

$$\dot{W}_{\text{elec,total}} = \dot{W}_{\text{elec,HT}} + \dot{W}_{\text{elec,LT}} + \dot{W}_{\text{pump}} + \dot{W}_{\text{fan}}. \tag{10}$$

Heat flux for the intermediate heat exchanger functioning as the condenser for the low-temperature side is given by [25]:

$$\dot{Q}_{\text{cond,LT}} = \dot{m}_{\text{ref,LT}}(h_2 - h_3). \tag{11}$$

The intermediate heat exchanger for the high-temperature side is used as an evaporator in the two-stage cascaded mode. Then, the evaporator heat flux is calculated by [26]:

$$\dot{Q}_{\text{cond,LT}} = \dot{Q}_{\text{evap,HT}} = \dot{m}_{\text{ref,HT}}(h_5 - h_8). \tag{12}$$

The expansion processes in an expansion device are assumed to be isenthalpic for both low- and high-temperature heat pump cycles. Therefore, the enthalpies before and after expansion are assumed to be constant:

$$h_4 = h_3, \qquad h_7 = h_8. \tag{13}$$

The useful condenser heating capacity is defined according to the formula:

$$\dot{Q}_{\text{cond,HT}} = \dot{m}_{\text{ref,HT}}(h_7 - h_6). \tag{14}$$

The cascaded refrigeration cycle COP is given by [26]:

$$COP_{\text{cycle}} = \frac{\dot{Q}_{\text{cond,HT}}}{\dot{W}_{\text{comp,LT}} + \dot{W}_{\text{comp,HT}}}. \tag{15}$$

Since heat losses in the heat exchangers of the cascaded system are not measured, the cascaded system COP is calculated according to Eq. (16):

$$COP_{\text{system}} = \frac{\dot{Q}_{\text{cond,HT}}}{\dot{W}_{\text{elec,total}}}. \tag{16}$$

The efficiency of the cascaded heat pump system in terms of the second law of thermodynamics is calculated by using a quality factor f_q [25]:

$$f_q = \frac{COP_{\text{system}}}{COP_{\text{limit}}}. \tag{17}$$

The limit COP associated with the Carnot reverse cycle heat source and sink is determined using the following formula [25]:

$$COP_{\text{limit}} = \frac{T_{\text{del}}}{T_{\text{del}} - T_{\text{amb}}}, \tag{18}$$

where T_{del} is the delivery temperature and T_{amb} is the ambient air temperature.

In addition, enthalpy and entropy values corresponding to the pressure and temperature required to calculate the system of Eqs. (1)-(18) are based on the CoolProp database. For closing the system of Eqs. (1)-(18), temperatures at the following points are defined [6]:

$$T_1 = T_{\text{amb}} - CAT_{\text{evap}}, \qquad T_7 = T_{\text{del}} - CAT_{\text{cond}}. \tag{19}$$

The compression ratios of the low-temperature and high-temperature cycles are given by the following equations:

$$P_{\text{ratio,LT}} = \frac{P_2}{P_1}, \qquad P_{\text{ratio,HT}} = \frac{P_6}{P_5}. \tag{20}$$

The system of Eqs (1)-(20) is solved by the Python code with CoolProp database, taking as input parameters the condenser heat flux $\dot{Q}_{cond-HT}$ =15 kW, delivery temperature T_{del}= +60 °C and varying T_{amb} ambient air temperature. The +60 °C delivery temperature was adopted in agreement with the standards in the CIS countries for a comfortable hot water supply. In the next section, the results of these calculations are shown for refrigerant pairs adapted to the climate of Kazakhstan.

Results and Discussion

As mentioned above, Kazakhstan has a sharp continental climate, particularly in its capital Astana, where the average monthly temperature is -15 °C during the heating season. On some days, the temperature may drop from -30 °C to -45 °C. Hence, for the low-temperature cycle, refrigerants with low boiling points (below -45 °C) were selected according to the data of Table 1. These considerations led us to select the following refrigerants pairs for the low and high-temperature cycles respectively: R410A/R290, R410A/R1234yf, R410A/R134a, R410A/R407C, R32/R290, R32/R1234yf, R32/R134a, R32/R407C, R404A/R290, R404A/R1234yf, R404A/R134a, R404A/R407C, R744/R290, R744/R1234yf, R744/R134a and R744/R407C.

The calculations based on the proposed mathematical model were carried out only for the first and third configurations operating in a two-stage cascade mode. In these configurations, the intermediate heat exchanger functions simultaneously as the condenser for the low-temperature stage and as the evaporator for the high-temperature stage.

Figures 5-8 show the variation of the system *COP* as the ambient temperature varies from -50 °C to +10 °C.

According to Fig. 5, the refrigerant pair R32/R134a exhibits the highest system *COP* among the configurations employing R32 in the low-temperature cycle; however, its operation is limited to ambient temperatures above -32 °C. In contrast, the R32/R290 pair ensures stable operation at lower ambient temperatures, down to -38 °C, with only a marginal decrease in performance. At an ambient temperature of +10 °C, the system *COP* values of R32/R134a and R32/R290 are 2.56 and 2.53, respectively, indicating comparable efficiency.

According to Fig. 6, the refrigerant pair R410A/R134a exhibits the highest system *COP* among configurations employing R410A in the low-temperature (LT) cycle, reaching a value of 2.54 at an ambient temperature of +10 °C. However, its performance decreases to a *COP* of 1.79 at -32 °C. At the lowest considered ambient temperature (-38 °C), the best performance among configurations with R410A in the LT cycle is achieved by the R410A/R290 pair, with a *COP* of 1.67.

The results presented in Fig. 7 indicate that the R404A/R134a refrigerant pair achieves a system *COP* of 2.51 at an ambient temperature of +10 °C, which decreases to 1.77 at -32 °C. Among the configurations employing R404A in the LT cycle,

Table 1 – Thermodynamic properties of the refrigerants considered in this study.

Refrigerant	Molecular mass	Critical temperature (°C)	Critical pressure (MPa)	Boiling point (°C)	ASHRAE code	ODP	GWP 100 yr
R32	52.02	78.2	5.80	-51.7	A2L	0	650
R134a	102.03	101.1	4.06	-26.1	A1	0	1430
R407C	86.20	86.4	4.63	-43.6	A1	0	1700
R410A	72.60	72.0	4.93	-51.5	A1	0	1890
R404A	97.61	72.07	3.73	-46.45	A1	0	3922
R290	44.10	96.7	4.25	-42.2	A3	0	20
R744	44.01	31.1	7.38	-78.4	A1	0	1
R1234yf	114.00	94.0	3.38	-30.0	A2L	0	4

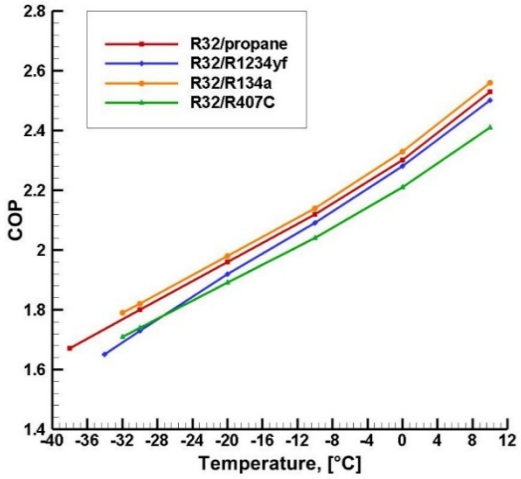

Figure 5 - System COP as a function of outdoor air temperature for R32-based refrigerant pairs.

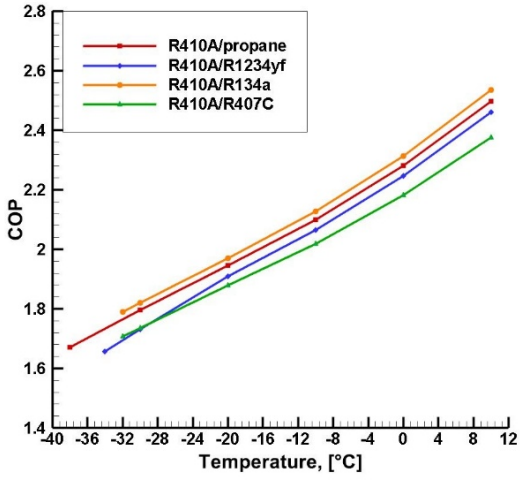

Figure 6 - System COP as a function of outdoor air temperature for R410A-based refrigerant pairs.

only the R404A/R290 pair is capable of operating at -37 °C, with a *COP* of 1.67.

The last four refrigerant pairs are capable of operating at an ambient temperature of -41 °C due to the use of low-boiling-point carbon dioxide (R744, -78.4 °C) in the LT cycle (see Fig. 8). Under these conditions, the highest system *COP* of 1.62 is achieved by the R744/R134a pair, while the R744/R290 configuration exhibits a slightly lower *COP* of 1.60.

The operational limits in terms of minimum ambient temperature and heating supply temperature (+60 °C) for the investigated refrigerant pairs are primarily governed by the permissible compression ratio, as defined in Eq. (20), for both the low- and high-temperature stages of the cascade heat pump. In practical applications, the compression ratio is typically limited to 9–10 to maintain compressor reliability and ensure efficient system performance [27]. Fig. 9 illustrates the relationship between system *COP* and the corresponding compression ratios for the analyzed refrigerant pairs.

The results presented in Fig. 9 correspond to an ambient temperature range from -30 °C to a heating supply temperature of +60 °C for a 15 kW air-to-water cascade heat pump operating in the first and third configurations.

According to Fig. 9, for the twelve refrigerant pairs excluding R744, the compressor in the LT stage operates near its maximum allowable limit, with compression ratios approaching 10

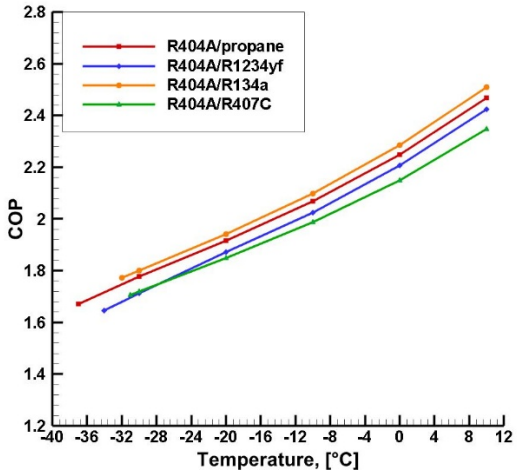

Figure 7 - System COP as a function of outdoor air temperature for R404A-based refrigerant pairs.

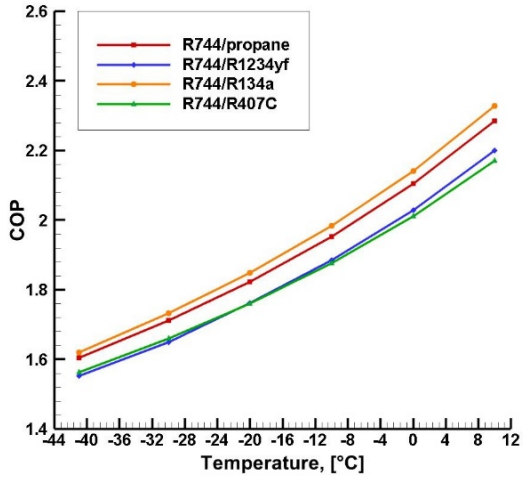

Figure 8 - System COP as a function of outdoor air temperature for R744-based refrigerant pairs.

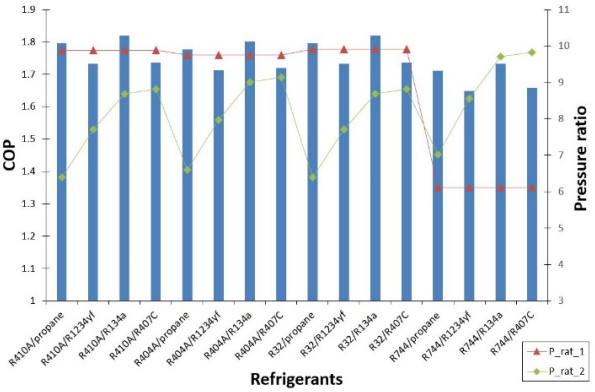

Figure 9 - Variation of the system COP and compression ratios for different refrigerant pairs.

[27]. Due to the lower heating capacity of the LT cycle compared to the HT cycle, the power consumption of the LT compressor remains lower than that of the HT compressor. Therefore, from a system efficiency perspective, it is advantageous to utilize the LT compressor as intensively as possible, thereby reducing the load on the more power-demanding HT compressor and improving the overall *COP*.

In contrast, for the four refrigerant pairs employing R744 in the LT cycle, the situation is reversed. Owing to the high critical pressure of R744, significantly higher compression work is required in the LT stage, necessitating more powerful compressors. As a result, shifting a greater portion of the load to the HT compressor becomes beneficial for enhancing system *COP*.

Furthermore, refrigerant pairs incorporating R290 (propane) exhibit relatively low compression ratios, which enables stable operation at lower ambient temperatures. In contrast, configurations using R407C and R134a in the HT cycle tend to operate close to the compressor capacity limits within the considered temperature range.

From an environmental perspective, the future applicability of the investigated refrigerant pairs is subject to increasingly stringent international regulations. The Montreal Protocol initiated global actions to protect the ozone layer by phasing out ozone-depleting substances; all refrigerant pairs considered in this study exhibit zero ozone depletion potential (ODP). Subsequently, the Kyoto Protocol introduced commitments to reduce greenhouse gas emissions, including high-global-warming-potential (GWP) refrigerants. More recently, the Paris Agreement established targets to limit global temperature rise to well below 2 °C, further strengthening the need for low-GWP alternatives.

In addition, the Kigali Amendment mandates a gradual phase-down of hydrofluorocarbon (HFC) refrigerants worldwide, with significant reductions scheduled from 2024 onward and long-term limits extending to 2036–2047 depending on country groups. In this context, high-GWP refrig-

erants such as R404A (GWP ≈ 3750), R410A (GWP ≈ 1890), R407C (GWP ≈ 1700), and R134a (GWP ≈ 1410) are expected to face progressive restrictions and eventual phase-down.

Consequently, current research and industrial trends are focused on the adoption of low-GWP synthetic refrigerants (e.g., R32, R1234yf, R1234ze) and natural refrigerants (e.g., R744 (CO_2), R717 (NH_3), and R290 (propane)). Among the refrigerant pairs analyzed in this study, several combinations demonstrate high thermodynamic performance, including R32/R134a, R410A/R290, R410A/R134a, R404A/R134a, and R744/R134a. However, due to environmental constraints, some of these pairs may only be considered transitional solutions. For instance, the R32/R290 pair can be regarded as an interim option because R32 still possesses a relatively high GWP (∼550).Although R290 (propane) demonstrates excellent thermodynamic performance and very low environmental impact, its flammability (ASHRAE safety classification A3) requires careful consideration in practical applications. The safe deployment of R290-based heat pump systems requires compliance with relevant safety standards, refrigerant charge limitations, proper ventilation, and leak prevention measures. Nevertheless, recent advances in system design and safety regulations have significantly increased the feasibility of using R290 in residential and commercial heat pump applications.

Overall, considering both environmental impact and system performance (COP), the R744/R290 refrigerant pair emerges as the most promising solution among the investigated options. This combination offers a favorable balance between low environmental impact and high thermodynamic efficiency, making it particularly suitable for future cascade air-source heat pump applications.

Configuration 1 achieves a system COP of approximately 2.0 with the lowest total power consumption among the three configurations. Configuration 2 shows a slightly lower COP (≈1.9) and increased power demand. Configuration 3 maintains a COP similar to Configuration 1 (≈2.0) but exhibits the highest total power consumption.

Overall, cascade heat pump configurations require about 47% higher electricity consumption compared to single-stage systems due to the operation of multiple compressors and increased system complexity.

The results show that the first and third configurations exhibit the highest efficiency in terms of *COP* across the considered ambient temperature range. The second configuration demonstrates a slightly lower efficiency, with a reduction of approximately 4.6% compared to the other two configurations. However, it offers practical advantages related to system assembly, installation, and operational flexibility. Notably, the second stage can be deactivated at ambient temperatures above -10 °C, enabling operation in a single-stage mode. Under these conditions, the system achieves considerable savings in electricity consumption while maintaining a relatively high *COP*.

At present, the authors have developed a laboratory-scale prototype of an air-to-water heat pump operating in Configuration 1, utilizing the refrigerant pair R410A/R134a. These refrigerants are widely available on the market and can be readily serviced under current conditions. The experimental setup is currently being used to conduct a series of performance tests and operational analyses.

Fig. 10 presents the real-time monitoring interface of the experimental setup. Key parameters displayed include indoor and outdoor temperature, relative humidity, and solar radiation intensity. The centralized data acquisition and control system enables continuous recording of all operating conditions, facilitating accurate monitoring and analysis throughout the experiments.

In addition, the integrated meteorological station allows for the incorporation of various renewable energy systems into the existing cascade heat pump prototype, such as solar thermal collectors, photovoltaic (PV) panels, solar concentrators, and wind turbines. This flexibility provides opportunities for future hybrid system in-

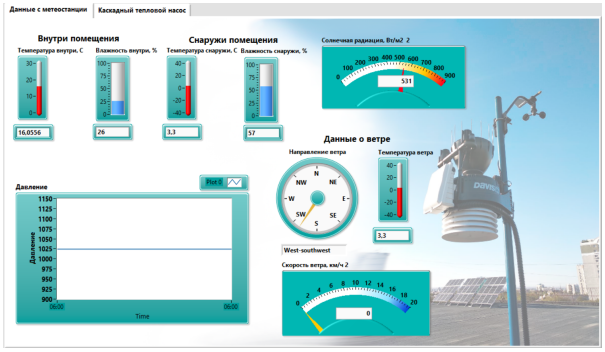

Figure 10 - Data monitoring interface of the meteorological station.

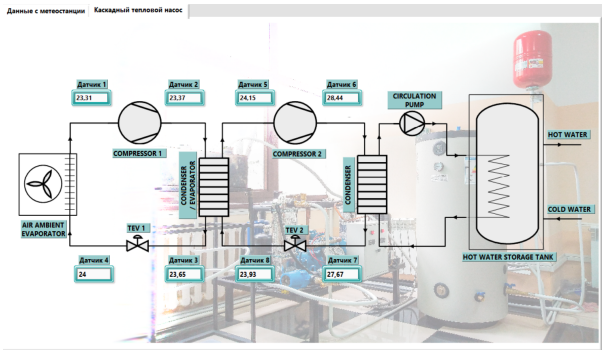

Figure 11 - Data monitoring interface of the cascade air-to-water heat pump system.

vestigations and enhances the applicability of the experimental platform for renewable energy integration studies.

Fig. 11 illustrates the design of the experimental cascade heat pump prototype, with eight temperature sensors installed at key locations within the system. The setup comprises two compressors, an air-source evaporator, a condenser, and an intermediate condenser–evaporator serving as the coupling between the low- and high-temperature circuits, two expansion valves (TEV 1 and TEV 2), a circulation pump, and a hot water storage tank.

In addition, the system is equipped with auxiliary safety components and piping arrangements, including pressure relief valves, check valves, filters, and instrumentation for pressure and flow control, ensuring safe, stable, and reliable operation during experimental testing.

Conclusions

This study evaluated the thermodynamic performance of three air-to-water cascade heat pump configurations using sixteen refrigerant pairs under cold climate conditions. The results show that R32/R134a and R410A/R134a achieve the highest COP, reaching up to 2.56 at +10 °C and about 1.98 at -30 °C; however, their applicability is limited by environmental constraints and operating range. Systems using R744 enable operation at extreme low temperatures down to -41 °C, with COP values of 1.62 (R744/R134a) and 1.60 (R744/R290).

The analysis confirms that compressor pressure ratio (≈9–10) is a key limiting factor, particularly in the low-temperature stage. Among the configurations, Configurations 1 and 3 demonstrate the highest efficiency (COP ≈ 2.0), while Configuration 2 shows a ∼4.6% lower COP but offers improved operational flexibility, including single-stage operation above -10 °C. Cascade systems exhibit approximately 47% higher electricity consumption compared to single-stage systems.

From an environmental and performance perspective, R32/R290 can be considered a transitional solution, whereas R744/R290 is identified as the most promising long-term refrigerant pair. Experimental validation using a developed prototype is ongoing, and future work will focus on low-GWP refrigerants and system optimization under real operating conditions.

Funding

This research is funded by the Committee of Science of the Ministry of Science and Higher Education of the Republic of Kazakhstan, Grant No. AP26102323 “Optimization of efficiency and configuration of high temperature heat pumps for integrating renewable energy sources and utilizing waste heat”.

Acknowledgements

The authors express their sincere gratitude to Professor Mohanraj Murugesan for long-standing collaboration in the field of heat pump technolo-

gies and their applications in space heating, domestic hot water production, desalination, drying, and other energy systems. The authors also gratefully acknowledge Professor Huasheng Wang for his valuable collaboration in the areas of heat transfer and thermodynamics, as well as in the integration of solar technologies with heat pump systems.

The authors would like to extend their appreciation to the "Heat Management" research team at the LEMTA R&D Center, University of Lorraine and CNRS (Nancy, France), in particular Professor Michel Feidt and Professor Olivier Botella for their continuous support and fruitful scientific discussions.

The authors also acknowledge the organizers and contributors of the double-degree Master's program between Al-Farabi Kazakh National University (Kazakhstan) and the University of Lorraine (France), "7M05405 – Mechanics and Energy," for their significant contribution to the academic training of Master's students.

Author Contributions: Conceptualization, Ye. Belyayev and Ye. Yerdesh; methodology, Ye. Yerdesh, A. Toleukhanov and Ye. Belyayev; software, Ye. Rymkul and Ye. Yerdesh; validation, Ye. Belyayev, M. Mohanraj, H.S. Wang, O. Botella and M. Feidt; formal analysis, Ye. Rymkul and Ye. Yerdesh; investigation, Ye. Rymkul, Ye. Yerdesh and A. Toleukhanov; writing-original draft preparation, Ye. Rymkul and Ye. Yerdesh; writing-review and editing, all authors; supervision, Ye. Belyayev, M. Mohanraj, H.S. Wang, O. Botella and M. Feidt. All authors have read and agreed to the published version of the manuscript.

REFERENCES

[1] Wang, Y., S. Zhang, Y. Gao, J. Liu, Z. Lin, and X. Zhang. "Recent advances in heat pump systems and key components: A comprehensive review." *Renewable and Sustainable Energy Reviews* 235 (2026): 116944.

[2] Ju, F., C. Xiao, W. Wu, J. Wu, H. Zheng, G. Li, X. Fan, and Y. Liu. "Experimental study on the performance of quasi-two-stage compression heat pump with r32/r1270 for district heating in cold regions." *Applied Thermal Engineering* 282 (2026): 128833.

[3] Mohanraj, M., Y. Belyayev, S. Jayaraj, and A. Kaltayev. "Research and developments on solar assisted compression heat pump systems - a comprehensive review (part a: Modeling and modifications)." *Renewable and Sustainable Energy Reviews* 83 (2018): 90–123.

[4] "Research and developments on solar assisted compression heat pump systems - a comprehensive review (part b: Applications)." *Renewable and Sustainable Energy Reviews* 83 (2018): 124–155.

[5] Cui, T., G. Ma, and L. Wang. "Research progress of co2 air source heat pump system for heating." *Renewable Energy* 259 (2026): 125083.

[6] Yerdesh, Y., Z. Abdulina, A. Aliuly, Y. Belyayev, M. Mohanraj, and A. Kaltayev. "Numerical simulation on solar collector and cascade heat pump combi water heating systems in kazakhstan climates." *Renewable Energy* 145 (2020): 1222–1234.

[7] Yerdesh, Y., A. Toleukhanov, M. Mohanraj, H. S. Wang, O. Botella, M. Feidt, and Y. Belyayev. "Air-to-water cascade heat pump thermal performance modelling for continental climate regions." *Entropie Thermodynamique - Energie - Environnement - Economie* 3 (2022): 1–16.

[8] Yang, J., C.-Y. Lee, J. Muehlbauer, and Y. Hwang. "Advanced defrosting techniques in air source heat pumps: A review of vapor injection, thermal energy storage, and experimental frost accumulation data." *Energy* 340 (2025): 139262.

[9] Wang, R., H. Yan, D. Wu, J. Jiang, and Y. Dong. "High temperature heat pumps for industrial heating processes using water as refrigerant." *Energy* 313 (2024): 133847.

[10] Hoang, D. K., T. G. Walmsley, D. J. Cleland, Q. Chen, and J. K. Carson. "Thermo-economic investigation and multi-objective optimization of cascade high temperature heat pump using low global warming refrigerants." *Applied Thermal Engineering* 279 (2025): 127901.

[11] Yang, L., X. Wang, B. Xu, and Z. Chen. "Where and how to place the injection structure of a cascade high-temperature heat pump with large-temperature differences: A comprehensive analysis." *International Journal of Refrigeration* 186 (2026): 106886.

[12] Boahen, S., S. K. Anka, K. H. Lee, and J. M. Choi. "Performance characteristics of a cascade multifunctional heat pump in the winter season." *Energy and Buildings* 253 (2021): 111511.

[13] Li, R., Y. Zhu, Y. Yang, K. Li, R. Zhang, J. Sun, and Z. Sun. "The effects of the opening of the electronic expansion valve in the high-stage cycle on the performance of a cascade heat pump water heater." *Journal of Building Engineering* 42 (2021): 103015.

[14] Le, K. X., M. J. Huang, N. N. Shah, C. Wilson, P. M. Artain, R. Byrne, and N. J. Hewitt. "Techno-economic assessment of cascade air-to-water heat pump retrofitted into residential buildings using experimentally validated simulations." *Applied Energy* 250 (2019): 633–652.

[15] Zhang, H., X. Geng, S. Shao, C. Si, and Z. Wang. "Performance analysis of a r134a/co2 cascade heat pump in severe cold regions of china." *Energy* 239 (2021): 122651.

[16] Zou, H., X. Li, M. Tang, J. Wu, C. Tian, D. Butrymowicz, Y. Ma, and J. Wang. "Temperature stage matching and experimental investigation of high-temperature cascade heat pump with vapor injection." *Energy* 212 (2020): 118734.

[17] Wu, Z., X. Wang, L. Sha, X. Li, X. Yang, X. Ma, and Y. Zhang. "Performance analysis and multi-objective optimization of the high-temperature cascade heat pump system." *Energy* 223 (2021): 120097.

[18] Ma, X., Y. Du, Y. Wu, B. Li, and C. Zhang. "Enhanced thermal output from air-source cascade heat pumps configuration for steam generation." *Case Studies in Thermal Engineering* 75 (2025): 107112.

[19] Wu, D., J. Jiang, B. Hu, R. Z. Wang, and Y. Sun. "Experimental investigation and industrial application of a cascade air-source high temperature heat pump." *Renewable Energy* 232 (2024): 121094.

[20] Sokolov, Y. Y. and B. M. Brodyanskyi. *Energy fundamentals of heat transformation and cooling processes*. Moscow: Energoizdat, 1981, book in Russian.

[21] Koshkin, N. N., I. A. Sakun, Y. M. Bambushek, N. N. Buharin, Y. D. Gerasimov, A. Y. Ilyin, V. I. Pekarev, A. K. Stukalenko, and L. S. Timofyevskyi. *Refrigeration machines and installations*. Leningrad: Mechanical Engineering Publisher, 1985, book in Russian.

[22] Trubayev, P. and B. Grishko. *Heat Pumps: Tutorial*. Belgorod BSTU Publisher, 2010, book in Russian.

[23] Kim, D. H. and M. S. Kim. "The effect of water temperature lifts on the performance of cascade heat pump system." *Applied Thermal Engineering* 67 (2014): 273–282.

[24] Song, Y., D. Li, F. Cao, and X. Wang. "Theoretical investigation on the combined and cascade co2/r134a heat pump systems for space heating." *Applied Thermal Engineering* 124 (2017): 1457–1470.

[25] Feidt, M. *Finite Physical Dimensions Optimal Thermodynamics I-II*. Elsevier ISTE Press Ltd, 2018, book in two editions. ISBN 978-1-78548-233-5.

[26] Ma, X., Y. Zhang, X. Li, H. Zou, N. Deng, J. Nie, X. Yu, S. Dong, and W. Li. "Experimental study for a high efficiency cascade heat pump water heater system using a new near-zeotropic refrigerant mixture." *Applied Thermal Engineering* 138 (2018): 783–794.

[27] Tsoi, A. and I. Kim. *Refrigeration Technology and Cold Consumer Technology: Tutorial*. Almaty: SK-print LLP Publisher, 2012, book in Kazakh/Russian. ISBN 978-601-263-174-6.

Information about authors

Ye. Rymkul *– Department of Mechanics, Farabi University, Almaty, Kazakhstan; Department of Mechanical Engineering, Satbayev University, Almaty, Kazakhstan.*

Ye. Yerdesh *– Department of Mechanics, Farabi University, Almaty, Kazakhstan; Department of Mechanical Engineering, Satbayev University, Almaty, Kazakhstan.*

A. Toleukhanov *– Department of Mechanical Engineering, Satbayev University, Almaty, Kazakhstan.*

Ye. Belyayev *– Department of Mechanics, Farabi University, Almaty, Kazakhstan; Department of Mechanical Engineering, Satbayev University, Almaty, Kazakhstan; e-mail: yerzhan.belyaev@kaznu.edu.kz; yerzhan.belyayev@gmail.com.*

M. Mohanraj *– Department of Mechanical Engineering, Hindusthan College of Engineering and Technology, Coimbatore, India.*

H.S. Wang *– School of Engineering and Materials Sciences, Queen Mary University of London, UK.*

O. Botella *– Universite de Lorraine, CNRS, LEMTA, F-54000 Nancy, France.*

M. Feidt *– Universite de Lorraine, CNRS, LEMTA, F-54000 Nancy, France.*